Highlights of Spanish Astrophysics XII, Proceedings of the XVI Scientific Meeting of the Spanish Astronomical Society held on July 15 - 19, 2024, in Granada, Spain. M. Manteiga, F. González Galindo, A. Labiano Ortega, M. Martínez González, N. Rea, M. Romero Gómez, A. Ulla Miguel, G. Yepes, C. Rodríguez López, A. Gómez García and C. Dafonte (eds.), 2025

Understanding the role of galaxy interactions in the Early Universe with MIRI/JWST observations of 'Big Three Dragons', a galaxy merging system at redshift z=7.15

Prieto-Jiménez, C.[1] **and MIRI European Consortium**

[1] Centro de Astrobiología (CAB), CSIC-INTA, Ctra. de Ajalvir km 4, Torrejón de Ardoz, E-28850, Madrid, Spain
cprieto@cab.inta-csic.es

Abstract

We present MIRI/JWST medium resolution spectroscopy (MRS) and imaging (MIRIM) observations of B14-65666, a Lyman-break galaxy (LBG) at a redshift of z=7.15. Also referred to as 'Big Three Dragons', B14-65666 was discovered in 2014. The HST rest-frame UV imaging revealed two resolved clumps, indicating that B14-65666 is a merging galaxy system. While this source does not exhibit any signs of active galactic nucleus (AGN) activity, it is one of the UV-brightest starburst galaxies in the Epoch of Reionization (EoR). This galaxy is one of the few where dust continuum emission has been detected in the EoR. MIRI/JWST data allow us to spatially and spectrally resolve the Hα emission in the different components of the merging system. Combined with the multiwavelength ancillary data, MIRI observations enable us to calculate physical properties, such as the star formation rate. The MIRIM F560W observations provide the resolved and integrated rest-frame optical continuum ($\approx$0.55μm). The combination of the MRS and MIRI data allows us to derive Hα equivalent width and confirm that the system is dominated by a young stellar population. This new MIRI/JWST study of B14-65666 will contribute in shading light on understanding the role of galaxy interactions in the early evolution of galaxies and reionization of the Universe.

1 Introduction

The James Webb Space Telescope (JWST) is revolutionizing our understanding of the formation and evolution of galaxies, particularly during the first gigayear after the Big Bang, with a special focus at the Epoch of Reionization (EoR). JWST has significantly expanded our understanding of the early Universe, photometrically identifying galaxy candidates up to redshift 16 and spectroscopically confirming galaxies up to redshift 14.2.

At the redshifts of the EoR, rest-frame optical emission lines move to the mid-infrared (mid-IR). The Mid-IR Instrument (MIRI) onboard the JWST has a spectral range from 4.9 to 28 μm, being able to detect optical emission lines. The Hα line is the Balmer line least affected by internal extinction, so it can be a useful tracer of the instantaneous star formation rate (SFR).

Most of the sources identified at the EoR are star-forming galaxies, but AGNs have also been discovered [16]. Higher number of galaxy mergers have been observed at higher redshifts than at lower ones, thus, it is expected that these systems have an important impact on galaxy evolution [12]. The gravitational forces from mergers can cause significant disruptions in galaxy structures and movements, leading to features such as tidal tails. These disturbances can cause gas to flow from the outer regions into the center of galaxies, triggering the formation of new stars in central areas [13].

The combination of the rest-frame UV to Far-IR spectroscopy and imaging observations is essential to study the complex coevolution between stars, gas, and dust in galaxies at high-z. However, only a few merging systems have the rich multi-wavelength observations to perform that studies [1].

2 Galaxy B14-65666

B14-65666 was discovered based on wide-field imaging data from the UltraVISTA survey in the COSMOS field [5]. It was then spectroscopically confirmed in Lyα [9]. Hubble Space Telescope high-angular imaging observations (F140W) identified two clearly separated components in the rest-frame ultraviolet, suggesting that the system is undergoing a merging event [6]. Observations performed with Atacama Large Millimeter/submillimeter Array (ALMA) in band 6 reported the detection of a 160 μm dust continuum and follow-up observations allowed the detection of [OIII] 88 μm, [CII] 158 μm, and underlying dust continuum emission at 90 μm, in Bands 6 and 8 [3] [10]. Furthermore, the [OIII] 88 μm and [CII] 158 μm are spectrally and spatially resolved into two components that could be associated with each of the UV components confirming that they are kinematically separated. The latest results made by JWST NIRCam revealed the complex morphology of two galaxy components: galaxy A, which consists of a compact core, surrounded by diffuse, extended, rest-frame optical emission, and galaxy B which has an elongated morphology composed of various individual clumps [15]. B14 is an ideal galaxy to study as it is an interacting merging system at the Epoch of Reionization and it has one of the richest multi-wavelength datasets from UV to IR.

3 Analysis and results

We present new JWST/MIRI imaging and medium spectral resolution integral field spectroscopy of B14-65666, galaxy at z=7.15. These new observations cover the 5.6 μm and the Hα emission line. Here, we do not explain how the data has been processed or calibrated. For details in the calibration and analysis refer to the article Prieto-Jiménez et al. in prep. To complete the study, we use ancillary data from NIRCam (filters F115W, F150W, F200W, F277W, F356W and F444W [15]), to trace the rest-frame UV and optical (see figure 1), and ALMA bands 6, 7 and 8 ([10], [14]), to trace the dust emission and FIR emission lines.

3.1 MIRI integral field spectroscopy

MIRI spectroscopy spatially and spectrally resolves the Hα emission in the system (see Figure 1). We extract the Hα spectra over the integrated galaxy system (total) and in the individual galaxy components (A and B). The apertures used are shown in Figure 1.

The Hα spectra of the total galaxy, and the A and B galaxy components are shown in Figure 2. We have performed a one-component Gaussian fit to derive the physical parameters. The observed Hα line is centered at a wavelength of 5.3510 $\pm$ 0.0004 μm corresponding to a redshift of 7.1513 $\pm$ 0.0007. The Hα line is spectrally resolved presenting an intrinsic full-width half maximum (FWHM) of 415 $\pm$ 86 km s^{-1} and a total observed flux of (23.1 $\pm$ 3.1) $\times 10^{-18}$ erg s^{-1} cm^{-2}. The Hα flux has been corrected for aperture losses, assuming that the two galaxies are unresolved at the MRS angular resolution, and by the contamination of the companion galaxy. The individual galaxy components (A and B) present an offset in velocity of 175 $\pm$ 28 km s^{-1}, in agreement with the one observed from FIR emission lines. The final redshifts, FWHMs, and fluxes are given in Table 1 for all galaxy components.

The instantaneous SFR, reported in Table 1 is derived directly from the Hα flux, obtaining a value for the total galaxy of 78 $\pm$ 11 $M_{\odot}$ yr^{-1}. Combining the Hα with the FIR dust continuum, the total SFR is 122 $^{+36}_{-18}$ $M_{\odot}$ yr^{-1} suggesting that 36 % of the star formation is obscured by dust in the system.

3.2 NIRCam and MIRI imaging

Galaxy A is composed of a dominant compact core and a faint extended emission characterized by an effective radius of 63 pc (0.012 arcsec). Galaxy B has a more clumpy elongated structure. Both galaxy components are surrounded by a diffuse, extended emission that could be associated to tidal tails. The MIRIM F560W photometry has been calculated following the same apertures than for the MRS Hα spectra. MIRIM F560W traces the rest-frame optical emission at 5.6μm and the Hα emission. The final observed flux is 0.93 $\pm$ 0.14 μJy. The MIRIM F560W fluxes for galaxies A and B are calculated by applying a similar methodology. Results are presented in Table 1.

We estimate the rest-frame equivalent width of $H\alpha$ from the F560W and $H\alpha$ fluxes. We measure the rest-frame optical (0.55 μm) continuum by subtracting the contribution of the $H\alpha$ line to the F560W flux. The rest-frame equivalent width of $H\alpha$ is derived by the ratio between the Hα flux and the continuum flux under the Hα. We obtain an $EW_0 = 437 \pm 65$ Å, which suggests a star formation over the last 50 Myrs, if constant stellar formation history is assumed, or a mixture of mature ($>$ 100Myrs) and young ($<$ 10Myrs) stellar populations.

We also combine the MIRI image with the NIRCam images (F115W, F150W, F200W, F277W, F356W, F444W). To do so, we matched the point spread functions (PSFs) of the images to that of the MIRI Image F560W by kernel convolution (Figure 1). With the photometric fluxes of these images, together with the photometric fluxes of MIRI F560W, ALMA

Bands 6, 7, 8 and the emission lines $H\alpha$ and [OIII]88 μm continuum, we model the Spectral Energy Distribution (SED) of the galaxy. We perform the fit using the code CIGALE [7]. The star formation history reveals that the galaxy can be modeled by a young constant stellar formation, with an instantaneous mature burst.

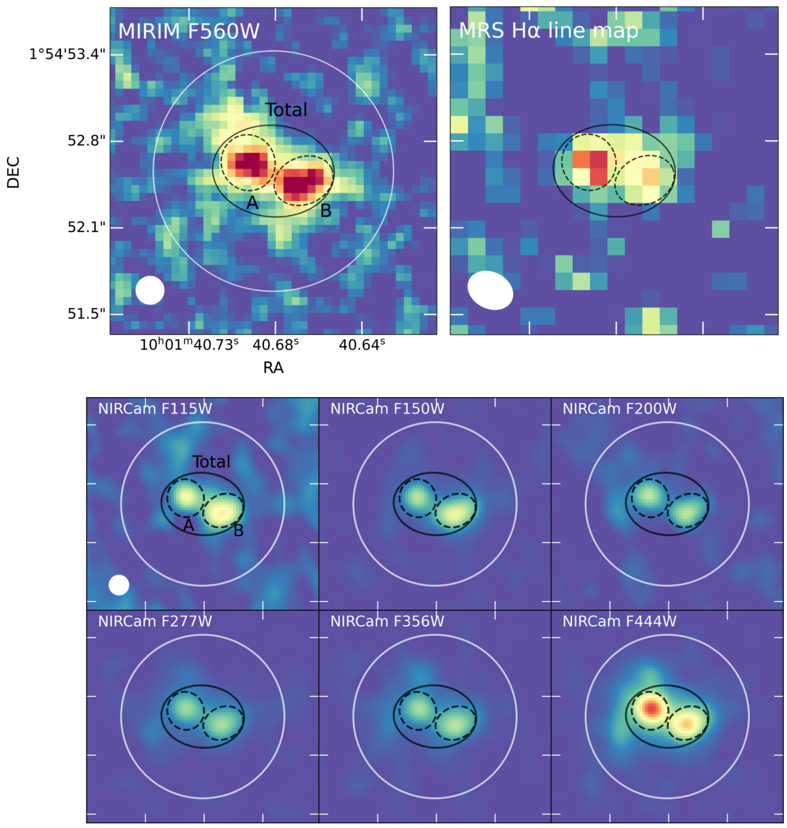

Figure 1: *Top left*: MIRI Image F560W. The black solid elliptical line represents the total aperture for the Hα emission of the whole galaxy, the black dotted lines represents the apertures for galaxies A and B respectively. The white circle area on the bottom left represents the spatial resolution (PSF FWHM) of MIRI Image F560W. *Top right*: Hα Line map. The white area represents the PSF FWHM of the MRS. *Bottom*: NIRCam cutouts in the filters, from left to right and top to bottom, 115, 150, 200, 277, 356, 444 W, homogenized to the PSF of MIRI Image, represented with the white circle on NIRCam Image F115W.

4 Conclusions

We have carried out the spectroscopic and imaging analysis of B14-65666 using new data from the MRS combined with the photometric analysis from MIRIM and NIRCam and we obtained the first detection of the Hα emission line in the galaxy B14-65666.

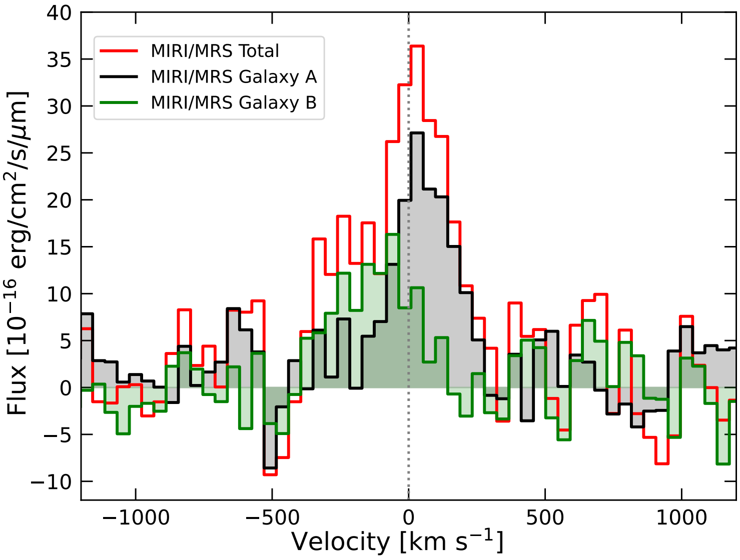

Figure 2: Hα spectra shown in velocity space for the two spatially separated galaxies, A and B (black line and green line respectively), identified in the Hα line map (Fig.1, top right). Red line shows the integrated MRS spectrum of B14-65666 extracted using the total aperture.

The Hα line traces the instantaneous star formation in galaxies. In the case of B14-65666, the Hα emitting gas reveals a complex structure that is dominated by two distinct clumps that are both kinematically and spatially separated. Also, it is found to be significantly attenuated by dust, which has implications for understanding the galaxy's SFR. Dust absorption of Hα indicates that the SFR is likely underestimated from Hα alone, as a significant portion of the star formation is obscured by dust.

The analysis also shows that B14-65666 has a relatively low EW of Hα, which suggests a mix of both young and mature stellar populations. This implies that B14-65666 has been forming stars over an extended period, not just in a recent burst of star formation. The SED modeling further supports this, indicating the presence of both younger, recently formed stars, as well as older stars.

B14-65666 is a crucial object for studying the process of stellar buildup in galaxies, particularly during major mergers. The observed two clumps of Hα emitting gas likely indicate an ongoing or recent merger event, making this galaxy an excellent case study for understanding how mergers contribute to galaxy growth and mass assembly during the EoR. However, to better understand the role of mergers in galaxy evolution at such high redshifts, it is essential to study a large sample of merging galaxies.

In summary, B14-65666 is a galaxy that offers valuable insights into the processes of star formation and galaxy assembly during the EoR. Its structured Hα emission, dust attenuation, and mixed stellar populations underscore the importance of mergers in the growth of early galaxies.

Table 1: Spectroscopic and imaging parameters derived for B14-65666.

Parameter	Total galaxy	Galaxy A	Galaxy B
Redshift	7.1513 ± 0.0007	7.1529 ± 0.0004	7.1481 ± 0.0007
FWHM [km s^{-1}]	415 ± 86	256 ± 41	323 ± 44
Flux Hα [$\times 10^{-18}$ erg s^{-1} cm^{-2}]	23.1 ± 3.1	11.9 ± 1.3	8.6 ± 1.2
Hα centroid [μm]	5.3510 ± 0.0004	5.3520 ± 0.0003	5.3489 ± 0.0004
Hα luminosity [$\times 10^{42}$ erg s^{-1}]	14.4 ± 2.0	7.4 ± 0.0	5.3 ± 0.7
SFR_{H_α} [$M_\odot\,yr^{-1}$]	77.6 ± 11.03	40.0 ± 4.7	28.7 ± 4.2
Flux MIRIM F560W [μJy]	0.929 ± 0.144	0.211 ± 0.009	0.215 ± 0.008

Acknowledgments

C.P-J., J.A-M and M.P acknowledge support by grant PIB2021-127718NB-100 from the Spanish Ministry of Science and Innovation/State Agency of Research MCIN/AEI/10.13039/501100011033 and by "ERDF A way of making Europe".

References

[1] Álvarez-Márquez, J., Colina, L., Crespo Gómez, A., et al. 2024, Astronomy and Astrophysics, 686

[2] Baraffe, I., Chabrier, G., Gallardo, J. 2009, ApJ, 702, 27

[3] Bowler, R. A. A., Bourne, N., Dunlop, J. S., et al. 2018, Monthly Notices of the Royal Astronomical Society, 481, 1631

[4] Bowler, R. A. A., Cullen, F., McLure, R. J., Dunlop, J. S., and Avison, A. 2021, Monthly Notices of the Royal Astronomical Society, 510, 5088

[5] Bowler, R. A. A., Dunlop, J., McLure, R., et al. 2014, Monthly Notices of the Royal Astronomical Society, 440, 2810

[6] Bowler, R. A. A., Dunlop, J. S., McLure, R. J., and McLeod, D. J. 2017, Monthly Notices of the Royal Astronomical Society, 466, 3612

[7] Boquien, M., Burgarella, D., Roehlly, Y., et al. 2019, Astronomy and Astrophysics, 622, A103

[8] Chabrier, G., & Baraffe, I. 2007, The Astrophysical Journal, 661, L81

[9] Furusawa, H., Kashikawa, N., Kobayashi, et al. 2016, The Astrophysical Journal, 822, 46

[10] Hashimoto, T., Inoue, A. K., et al. 2019, Publications of the Astronomical Society of Japan, 71

[11] Hashimoto, T., Inoue, A. K., Sugahara, Y., et al. 2023, The Astrophysical Journal, 952, 48

[12] Rodriguez-Gomez, V., Genel, S., Vogelsberger, M., et al. 2015, Monthly Notices of the Royal Astronomical Society, 449, 49–64

[13] Spilker, J., Justin S., Hayward, Christopher C., et al. 2022, The Astrophysical Journal, 929, 1

[14] Sugahara, Y., Inoue, A. K., Hashimoto, T., et al. 2021, The Astrophysical Journal, 923, 5

[15] Sugahara, Y., Álvarez Márquez, J., Hashimoto, T., et al. 2024, arXiv e-prints

[16] Yang, G., Caputi, K.I., Papovich, C. et al. 2023, The Astrophysical Journal, 950, 1, L5